RISØ

Risø-R-Report

Summary report: The shadow effect of large wind farms: measurements, data analysis and modelling

Sten Frandsen, Rebecca Barthelmie, Ole Rathmann, Hans E. Jørgensen, Jake Badger, Kurt Hansen, Søren Ott, Pierre-Elouan Rethore, Søren E. Larsen, Leo E. Jensen

Risø-R-1615(EN)

Risø National Laboratory
Technical University of Denmark
Roskilde, Denmark
October 2007

DTU

Author: Sten Frandsen
Title: The shadow effect of large wind farms
Department: Wind Energy

Risø-R-1615(EN)
July 2007

Abstract (max. 2000 char.):

It was the goal of the project – by means of data from the demonstration wind farms Horns Rev and Nysted, analyses of these data and modelling – to facilitate prediction of the power losses from a wind farm should a new wind farm be built upwind relative to the prevailing wind direction. Or conversely, predict with adequate accuracy the production of a new wind farm built downwind of an existing wind farm.

The project should be seen in the perspective of the two existing demonstration wind farms that extend 5-10 km in each direction. In order to e.g. use the existing electrical infrastructure it may appropriate to build new wind farms rather close to the existing wind farms. A relevant question is therefore how far away new wind farms must be placed to avoid too large power losses.

Measurements have been carried out for several years at the two sites, and databases have been prepared. The databases – one for each site – include production and operational statistics for the wind turbines and statistics for the meteorological measurements carries out in the vicinity of the wind farms.

Several different modelling activities were carried out, which *intentionally* to some extent are redundant. Thus, if different modelling efforts results in comparable results, the quality of the models will be tested outside the physical range where data are available.

All considered the project participants find that the project has been immensely successful. The main achievements of the project are:

- Measurements were carried out at the Nysted and Horns Rev demonstration wind farms for several years. Doing so included design, installation and operation of the measurement system
- A data base was built from the incoming data. The data have been organized to facilitate verification of the models developed as part of the project
- 6-7 different models have been developed and compared.
- Approximately 20 journal and conference papers have resulted directly from the project

ISSN 0106-2840
ISBN 978-87-550-3616-1

Contract no.:
Energinet.dk 6505

Group's own reg. no.:
(Føniks PSP-element)
1120144

Sponsorship:

PSO

Cover :

Pages: 34
Tables: 2
References: 25
Figures: 26

Information Service Department
Risø National Laboratory
Technical University of Denmark
P.O.Box 49
DK-4000 Roskilde
Denmark
Telephone +45 46774004
bibl@risoe.dk
Fax +45 46774013
www.risoe.dk

Contents

Preface

The report constitutes the final summary report of the project *Store mølleparkers skyggevirkning: malinger og dataanalyse*, financed by the Danish Public Service Obligation (PSO), project no. Energinet.dk 6505.

The project period was 15.9.2004 – 31.03.2007.

The participating organisations were Risø DTU, E2 and Elsam – the two latter now merged into DONG Energy.

The project has been "online" reported through its webpage:

http://teamsites.risoe.dk/stormaalepark

Access may be achieved by contacting the webpage's administrator Hans E. Jørgensen, hans.e.joergensen@risoe.dk

A significant amount of work has been done by the staff of DONG energy to prepare the measurements, carry out data acquisition, maintain the measurement system and to build data bases. In particular, Claus Perstrup and Paul B. Sørensen of DONG Energy should be mentioned and acknowledged for their contribution to the project.

1 Executive summary

1.1 Project objectives

It is the goal of the project – by means of data from the demonstration wind farms Horns Rev and Nysted, analyses of these data and modelling – to facilitate prediction of the power losses from a wind farm should a new wind farm be built upwind relative to the prevailing wind direction. Or conversely, predict with adequate accuracy the production of a new wind farm built downwind of an existing wind farm.

The project should be seen in the perspective of the two existing demonstration wind farms that extend 5-10 km in each direction. In order to e.g. use the existing electrical infrastructure it may appropriate to build new wind farms rather close to the existing wind farms. Relevant questions are therefore how far away new wind farms must be placed to avoid too large power losses and how these losses should be quantified by models or measurement in case of conflicting commercial interests.

1.2 Issues comparing models and measurements

There are some major issues in wind farm model validation studies which will be discussed below. As stated above we concentrate here on power loss modelling which should encompass the whole range of wind speeds and directions and we also consider that the range of wind farm/wake model extends from engineering through to full CFD models. In general, computing requirements for CFD models means we are restricted to examining a number of specific wind speed and direction cases and only a moderate number of turbines rather than wind farms with ~100 turbines which can easily be done by WindFarmer and WAsP. On the other hand it can be difficult to extract reasonable simulations from some of the wind farm models for very specific cases. For example, WAsP relies on having a Weibull fit to wind speed distributions and fairly large directional sectors (30°). Therefore for specific wind speeds and narrow directional bins models like WAsP are never going to produce very exact solutions because they are being used beyond their operational windows. In addition to this there are a number of specific issues:

- Establishing the freestream flow. The major issues in determining the freestream flow are the displacement of the measurement mast from the array (assuming there is a mast), adjustments in the flow over this distance especially in coastal areas and differences in height between the measurement and the turbine hub-height. If there is no mast or the mast is in the wake of turbines or subject to coastal flow then the turbine(s) in the freestream flow may be used. If power measurements are used to determine wind speed they will be subject to any errors in the site specific power curve.
- Wind direction, nacelle direction and yaw misalignment. Because of the difficulty in establishing true north when erecting wind vanes (especially offshore where landmarks may not be determinable) it can be difficult to establish a true freestream direction. Even a well maintained wind vane may have a bias of up to 5° and it is important to understand this because the total width of a wake may be of the order 10-15° at typical turbine spacing. In a large wind farm, each turbine may have a separate bias on the direction, which is difficult to determine. Analysis must be

undertaken to calibrate the maximum wake direction to within 1° and to check for bias of the yaw angle on each wind turbine in the array.

- If there is a gradient of wind speeds across the wind farm as there may be e.g. in coastal areas, near a forest or caused by topography these variations will need to be accounted for before wake calculations are undertaken.
- In terms of modelling wakes both the power curve and thrust coefficients must be known but these will vary according to the specific environment. A power curve must be calculated for the site. For modelling, the question of whether the thrust coefficient should be set to one value for the wind farm or at each individual turbine in each simulation is still an open one. The state-of-the-art is to validate the individual power and pitch curves with reference to the nacelle anemometer, which seems to be a rather robust method to determine changes in the system setup.
- Comparing the modelled standard deviation of power losses in a row with the measured standard deviation raises a number of issues. The two most important are ensuring that the time averaging is equivalent between models and measurements and taking into account that there will be natural fluctuations in the wind speed and direction in any period. Models are typically run for specific directions but it may be necessary to include the standard deviation of the wind direction in the model simulations.
- In the large wind farm context the time scale of wake transport must be considered. A large wind farm with 100 turbines in a 10 by 10 array with an 80 m diameter rotor and a space of 7 rotor diameters has a length of nearly 6 km. At a wind speed of 8 m/s the travel time through the array is more than 10 minutes. As mentioned above the wind direction will be subject to natural fluctuations in addition to possible wake deflection but there will also be natural variations in the wind speed over this time scale.
- Determining turbulence intensity and stability may be critical. Turbulence intensity is a key parameter in many models. Using either mast data to determine this information or deriving it from turbine data is subject to fairly large errors for the reasons discussed above and because the accuracy of temperature measurements used to derive stability parameters is often inadequate.

1.3 Measurements and data analyses

Measurements have been carried out for several years at the two sites, and databases have been prepared. The databases – one for each site – include production and operational statistics for the wind turbines and statistics for the meteorological measurements carries out in the vicinity of the wind farms.

Having the considerations of Section 1.2 in mind, the data have been analyzed in various ways by members of the project team. One particularly important type of result is the wind-speed-drop curves: by mean of the (inverse) power curve of the wind turbines the mean wind speed at each wind turbine position is derived and together with the met mast measurements, the development of wind speed through and downwind of the wind farm is estimated for Westerly winds. These wind-speed-drop curves are the main experimental results, which are paramount to the verification of the numerical and analytical models.

Also turbulence and vertical mean wind speed profiles are derived from the measurements and applied in connection with the modelling work.

In addition, so-called laser-lidar measurements have been performed, though with less conclusive result.

The measurements are reported in more details in Section 2.

A separate report on the measurements and basic data analysis will be issued within the next few months

1.4 Modelling

Although extremely valuable the data from the two demonstration projects, the data themselves are not sufficient to document the operational model(s) that is intended to emerge from this project.

Therefore, we started several different modelling activities, which *intentionally* to some extent are redundant. Thus, if different modelling efforts results in comparable results, the quality of the models will be tested outside the physical range where data are available.

The engineering models presently applied for calculating production losses due to wake effects from neighbouring wind turbines are based on local unit-by-unit momentum equations, disregarding a two-way interaction with the atmosphere, Frandsen et al. (2006). On the other hand, another group of models, which did not reach engineering maturity, predict the array efficiency of very large wind farms by viewing the wind turbines as roughness elements. A third option is to apply CFD[1] schemes. These models encompass the individual wind turbines and thus track and integrate the momentum and energy budget for the whole wind farm, but has hitherto not been applied for the two way interaction with the atmosphere.

A total of 6-7 different modelling approaches have been applied.

These are described in Section 3.

1.5 Conclusions

All considered the project participants find that the project has been immensely successful. The main achievements of the project are:

- Measurements were carried out at the Nysted and Horns Rev demonstration wind farms for several years. Doing so included design, installation and operation of the measurement system
- A data base was built from the incoming data. The data have been organized to facilitate verification of the models developed as part of the project
- 6-7 different models have been developed and compared. It is found that the modelling work already done forms a sufficient and adequate basis for prediction of production from one or more large wind farms
- Approximately 20 journal and conference papers have resulted directly from the project

1 Computational Fluid Dynamics – numerical solutions to the equations of motion of the fluid.

- A separate data analyses report to be issued in the fall of 2007. The report will include CD with main analysis results

Although we find that the available data and the modelling work already done are sufficient as scientific basis, the user software – anticipated in the project proposal – remains to be designed and produced. The task of integrating the small-scale and large-scale models proved more difficult than anticipated. However, we are confident that solutions will be found in the near future.

2 Data from Horns Rev and Nysted wind farms

The two demonstration wind farms were owned by ELSAM and E2, respectively, when the project was initiated. Presently, the Horns Rev wind farm is jointly owned by the power companies DONG Energy and Vattenfall, and the Nysted wind farm is owned by DONG Energy.

A separate report on the measurements and basic data analysis will be issued within the next few months.

2.1 Description of sites

The basic wind farms layout is described below.

a) Horns Rev

The wind farm layout is a 10 times 8 matrix forming a slightly oblique rectangle, Figure 1. The distance between the turbines is 560 meters in both directions, corresponding to 7 rotor diameters. The Vestas V80 wind turbine units have a rotor diameter of R=80m, and hub height H=70m.

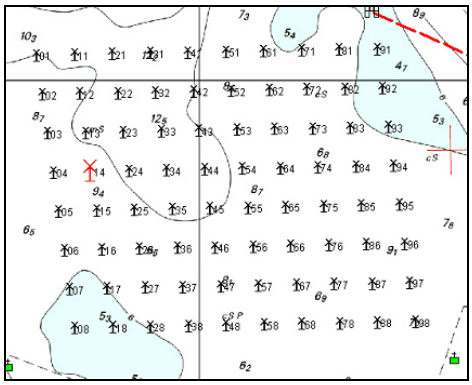

Figure 1 The turbines are numbered so that the westernmost column is numbered from 01 to 08 with 01 being the turbine in the northwest corner, and the easternmost column being numbered 91 through 98. This may lead to the wrongful assumption that there are actually 98 turbines, but as several numbers are unused, the number of turbines is still only 80.

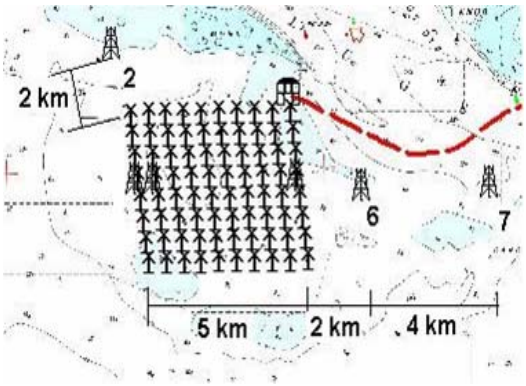

Figure 2 The position of the meteorological towers. The "downwind" met masts are off-line relative to the West-East wind turbine rows – placed on a line in the middle of two rows.

For the wake measurement, the most interesting turbine data are the diameter, the hub height and the thrust coefficient. Since the Vestas V80 turbine is a pitch-variable speed machine, running with constant tip-speed ratio at low to medium wind speeds, the thrust coefficient is fairly constant. This is very convenient for the scientific work as e.g. relative wind speed deficits can be expected to be fairly constant for a large wind speed range.

The power and thrust coefficient curves are specific to the turbines delivered for the Horns Rev wind farm and may not apply to V80 turbines delivered for other projects.

The wind farm is located in the North Sea, approximately 30 km west of Esbjerg. The distance to the nearest point on shore (Blåvands Huk) is approximately 13 km.

Around the wind farm three met masts are installed, Figure 2. The oldest mast is called M2. This mast was installed before construction of the wind farm and is the one that was used to determine the wind resource at the site. Several other papers have described and analysed measurements from that mast.

In the summer of 2003 two more masts (called M6 and M7) were installed, Figure 2. The purpose of these masts is to study the recovery of the shaddow flow behind the wind farm for westerly winds, and support the development of new scientific and engineering models for calculation of external wake effects from large offshore wind farms.

M2 is located 2 km north-northwest of the northwest corner turbine (01). M6 and M7 are located 2 and 6 km east of the wind farm respectively on a line that passes right through the middle of the fourth and fifth row.

In addition to the wind flow measurements in the met mast, statistics of power and other operational parameters from all wind turbine units were recorded.

b) Nysted

Nysted wind farm was commissioned in 2004 by Energi E2 and is now owned by DONG Energy. It has the largest installed capacity in an offshore wind farm, 165.6 MW. It is located approximately 11 km to the south of the island of Lolland, Denmark. There are 72 turbines laid out in nine rows, with west-to-east spacing of 10.5 rotor diameters (i.e. an inter-turbine distance of 857 m) and eight columns north to south with a spacing of 5.8 D (481 m), see Figure 3.

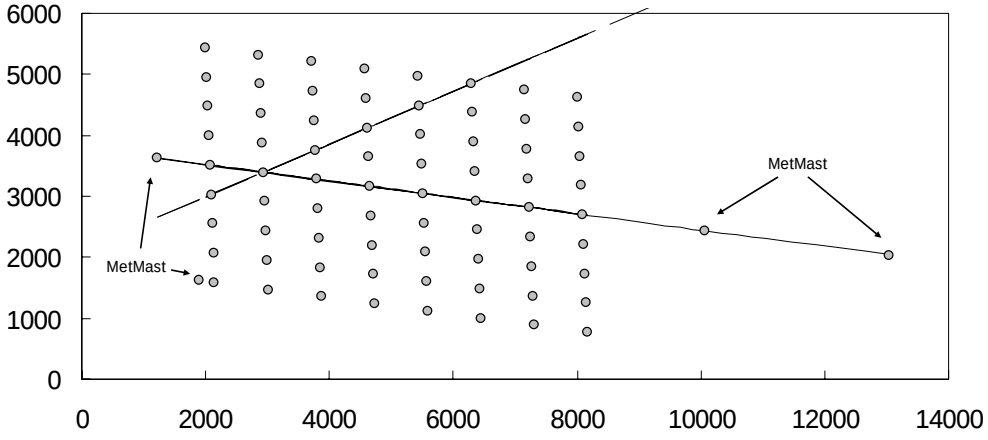

Figure 3. *Layout of the Nysted wind farm. Different wind directions offer different wind turbine separations for model verification. The "downwind" met masts are in line with wind turbine row..*

The turbines are Bonus 2.3 MW with a hub height of 68.8 m and a rotor diameter of 82.4 m. Prior to construction, two 50 m meteorological masts were erected to provide site wind assessment, one on-site, the other approximately 11 km east on the island of Falster

(Gedser land mast). After wind farm construction, four additional 70 m masts were erected. Two of these are close to or upwind of the wind farm in the prevailing south-westerly wind direction. The remaining masts are downwind of the array in the prevailing wind direction at distances of 2 and 6 km. Ten-minute averages of power, yaw and status signal from each turbine are available from June 2004 and onwards. Meteorological data were utilised from all four post-construction masts where wind speed profiles, direction and temperature measurements were selected from the SCADA database. Data collection within the SCADA system ensures that all data are time synchronised.

2.2 Measurements made

Globally, the amount of information available is satisfying. The data are stored as 10-minute statistics and some one-second statistical data was available on request. In both cases the relevant sensors available were the wind speed anemometers and wind vanes on the met masts and the wind turbine anemometers, the thermometers on the met masts, the power production sensors and the yaw direction sensors of the turbines. In addition, the pitch angle of the wind turbine blades and the rotor rotational velocity were used as quality filters.

While the whole data set at Nysted including additional parameters such as humidity were available, supplied data from Horns Rev were solely the requested variables described above. The data available from Horns Rev cover the year of 2005 (>50.000 data points), while Nysted data were available from June 2004 onwards (>150.000 data points).

The wind turbines were in both cases operating more than 97% of the time, which provides a fairly large amount of useable data. Nonetheless, the cases when the whole wind farms were operating at full capacity (all the turbine are working) are more limited (less than 10% of the time). This amount of data is not enough for making wake statistics, as it requires, on top of this condition, additional conditions over the wind direction and wind speed. In order to overcome this problem, the condition where a full row of turbines are working was used instead, which provide a much larger amount of data (>70%).

The two data sets were first available in two different data format: a SCADA database for Nysted, updated in real time, and a raw ASCII file format for Horns Rev. This required gathering the two formats in a new SQL database format.

2.3 Data quality

The quality of the two data sets is generally good. Globally, the amount of information available is satisfying in both cases. However, during the data analysis campaign, several types of data corruption were encountered.

In Nysted database, some of the mast wind vane sensors kept indicating the same wind direction during a relatively long period of time (sometimes several days), while the other wind direction sensors were all agreeing on a completely different wind direction. This seems to indicate that the wind vane could have been blocked physically during those periods, or that the data was corrupted, and reproducing the same values over and over. If it is the second explanation is the right one, it implies that there might be a similar corruption of data in other sensors, which was – however – not spotted during the data analysis.

In Horns Rev database,

- The yaw sensors of the wind turbines were in general of rather poor reliability. It seems that after a shut down, the yaw sensor is not working properly for a relatively long period of time (sometimes several hours).
- The mast 2, located north west of the wind farm, is equipped with 3 wind vanes, but during most of the year 2005, only one was working. During the second half of the year 2005, this sensor was indicating a wind direction covering just a fraction of the direction angles, while the two other masts were covering the full range of directions. This seems to indicate that the wind vane was physically blocked between two directions, or that the algorithm used to extract the data was deficient.
- The top anemometers at all the three met masts are all indicating a wind speed higher that it would be expected from a logarithmic profile. While it's a commonly observed problem, several interpretations can be found in the literature, arguing that the top anemometers are the only one to be trusted, or the opposite. According to a parallel study over a comparison between a LIDAR measurement located on the platform, and the met mast measurements, done at Risø DTU, the top anemometer seems to be over predicting the wind speed. Following these observations, the top anemometers were not considered in the data analysis.
- At least one wind turbine (WT93) seemed to have an offset of time (at least 30 min) during a relatively long period of time (at least a day). This was apparent on the power production, where the turbine was following the rest of its neighbouring turbines, with a small delay. This kind of data corruption is difficult to identify and it is possible that other cases of timestamp corruption have gone unnoticed.
- The wind farm was sometimes under power regulation, which means that the power output of the turbines did not follow the regular power curve. In order to exclude those cases from the data analysis, the timestamps when it occurred were referenced in a table. Nonetheless some cases seemed to be unreferenced, as they were sometime visible in the data. The power regulation can sometimes be very slight, which means that it could be possible that some cases were not spotted during the data analysis.

2.4 Data analyses

As stated previously, a separate data analysis report will be issued. The report will contain sets of tables and graphics of the wind speed development through the wind farm and downwind of the wind farm as well as other fundamental analyses. The results of these analyses will also be available on a CD.

3 Modelling efforts

Although extremely valuable the data from the two demonstration projects, the data themselves are not sufficient to document the operational model(s) that is intended to emerge from this project.

Therefore, we have started several different modelling activities, which *intentionally* to some extent are redundant. Thus, if different modelling efforts results in comparable results, the quality of the models will be tested outside the physical range where data are available.

The engineering models presently applied for calculating production losses due to wake effects from neighbouring wind turbines are based on local unit-by-unit momentum equations, disregarding a two-way interaction with the atmosphere, Frandsen et al. (2006). On the other hand, another group of models, which did not reach engineering maturity, predict the array efficiency of very large wind farms by viewing the wind turbines as roughness elements. A third option is to apply CFD[2] schemes. These models encompass the individual wind turbines and thus track and integrate the momentum and energy budget for the whole wind farm, but has hitherto not been applied for the two way interaction with the atmosphere. Another computational technique, *L*arge *E*ddy *S*imulation (LES), has a much finer spatial resolution and may therefore simulate the vortices shed from the blades and the subsequent breakdown of the vortices into chaotic eddies. The high resolution presently prohibits the application of LES for wind farms with hundreds wind turbines, but a special technique, where the simulated wake from a rotor is fed cyclically on to the same rotor, is presently being tested. While the method is not yet operational in the engineering sense, it may be used to emulate an infinite row of wind turbines, which is a key element of the first model presented below.

3.1 Analytical hybrid model

The analytical model in question is a computationally economic model-complex that links the small and large-scale features of the flow in wind farms. Thus, if successful it will be applicable for any size of wind farm. The model is being evaluated and adjusted and calibrated by means of measurements and the numerical techniques mentioned above. Further, the model is being numerically implemented, See Section 3.3.

As it is often needed for offshore wind farms, the analytical model[3] handles *a priori* a regular array-geometry with straight rows of wind turbines and equidistant spacing between units in each row and equidistant spacing between rows. Firstly, the base case with the flow direction being parallel to rows in a rectangular geometry is considered by defining three flow regimes. Secondly, when the flow is not in line with the main rows, solutions may be found for the patterns of wind turbine units emerging corresponding to each wind direction. The solutions are in principle the same as for the base case, but with different spacing in the along wind direction and different distance to the neighbouring rows.

Returning to the base case and counting from the upwind end of the wind farm, the model encompasses 3 main regimes as illustrated in Figure 4.

2 Computational Fluid Dynamics – numerical solutions to the equations of motion of the fluid.

3 The model presented in Section 3.3 handles any geometry.

In the first regime, the wind turbines are exposed to multiple-wake flow and an analytical link between the expansion of the multiple-wake and the asymptotic flow speed deficit are derived.

The second regime materializes when the (multiple) wakes from neighbouring rows merge and the wakes can only expand upward. This regime corresponds (but is not identical) to the flow after a simple roughness change of terrain.

The third regime is when the wind farm is "infinitely" large and flow is in balance with the boundary layer.

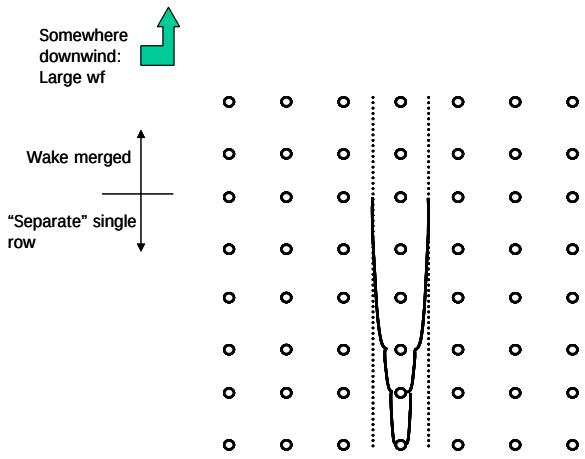

Figure 4. *Illustration of the regimes of the proposed model. The wind comes from the "South", parallel to the direction of the rows.*

Additional regimes need to be defined when the model is to be practically applied, i.e. the first row facing the wind is obviously not exposed to wake conditions, and most frequently the wake hits the ground before it merges with the wakes from the neighbouring rows. However, it is here chosen to disregard these in order to produce a clearer presentation. For the same reason and because it plays a lesser role than the mass momentum flux, the surface friction is disregarded in regimes 1 and 2, but not in regime 3. Should experimental evidence point to it, it is possible to include the surface blocking and stress in the model explicitly or implicitly by making the wake expansion and/or the growth of the internal boundary layer in regime 2 dependent on surface roughness.

The mathematical details are found in Frandsen et al (2006) and the effort to programme a more general version of the model is given in Section 3.3.

3.2 Extension of WA^{S}P

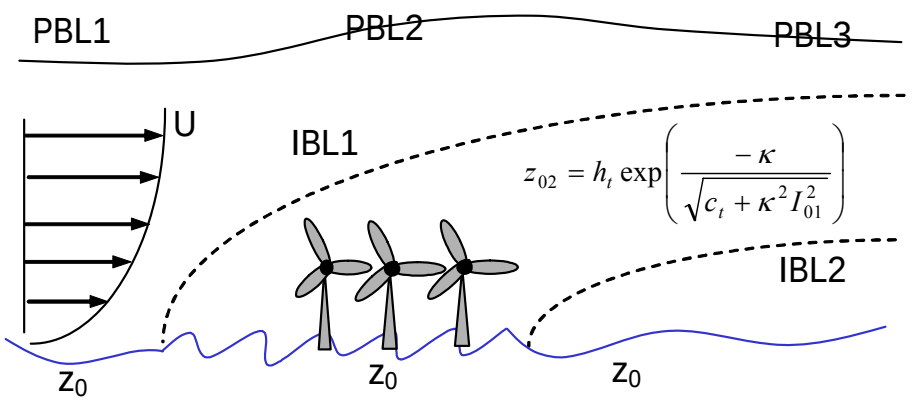

Figure 5. *Illustration of the added roughness approach to wind farm modelling.*

Given current understanding that wind farm models under-estimate wake losses in large offshore wind farms an alternative approach is to depict the wind farm as an area of higher roughness. This can be done either within the wind farm model using both wake modelling and the added roughness layer or within a simple 2-dimensional model. In the 2D model the roughness element causes an internal boundary layer to grow over the wind farm. The area of higher roughness causes the wind speed at hub-height to increase. After the wind farm when the roughness returns to an open sea value (either an abrupt change or with an exponential decay) the wind speed is allowed to recover. The impact on wind speed is dictated by the wind farm thrust coefficient and the spacing of the turbines in the wind farm.

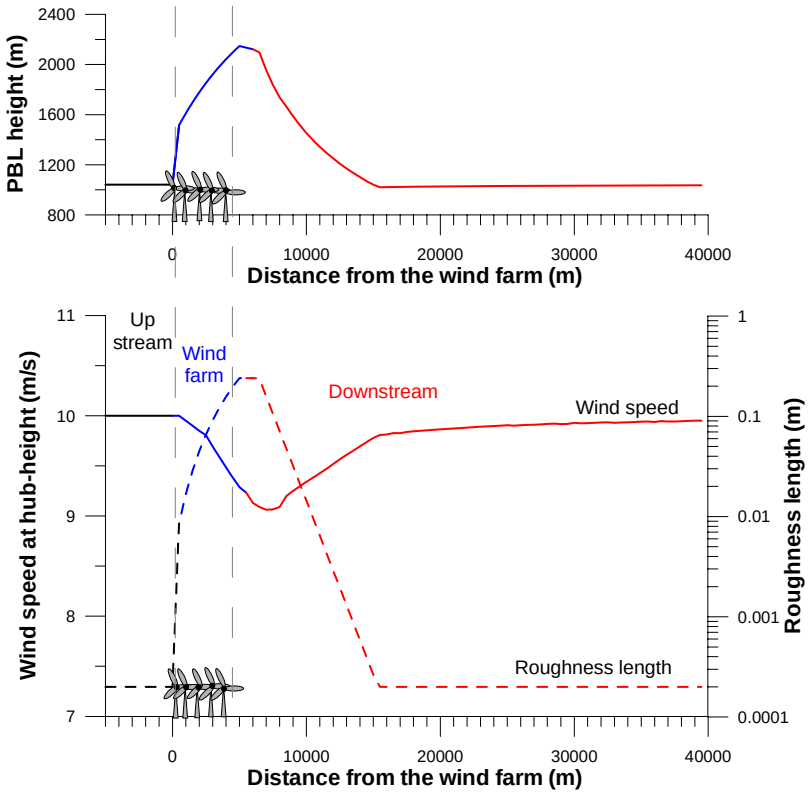

Figure 6. *Results from the added roughness model*

As shown in Figure 6, the impact of the wind farm is estimated to be advected at least 10 km downstream. Results of comparison of this approach with standard wake modelling in WAsP indicates that using higher roughness areas allows longer for the atmosphere to recover from the impact of wind farms taking 6-8 km for hub-height wind speeds to recover to 98% of their initial value. This is in line with results from CFD modelling.

Model	Distance in km for wind recovery (to 98% of its initial value)
WAsP z0(block) 0.1 m	6
WAsP z0(block) 0.5 m	7

WAsP z0(block) 1.0 m	8
WAsP wake decay 0.075	2
WAsP wake decay 0.05	3
Added roughness: exponential z0 decay	14 (5%-7.5)
Added roughness: constant z0	14 (5%-5.5)
EMD CFD model: z0 0.1-0.5 m	8
EMD CFD model: z0 1 m	7

Discussion of the application of the Simple WAsP-like models

Above, the wind shadows behind larger wind farms are estimated, using versions of the roughness change models, applied in the WAsP program. We shall discuss the possibilities a little closer, comparing with the data, obtained in the observation program, described and discussed in Section 2, and in further details in the separate data report to be issued later.

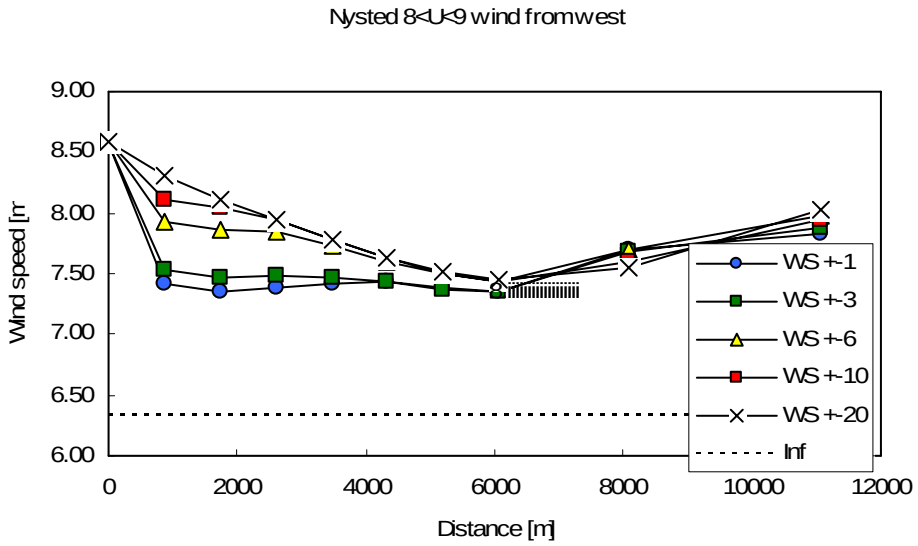

Figure 7. *Variation of the mean speed through and behind the wind farm at Nysted, at hub height 70 meter. The different curves correspond to the number of wind angle sectors enters into the averaging.*

Figure 7 illustrates that the wind speed behind the farm divided by the upstream wind are pretty robust, and can be taken as: 0.86, 0.88 and 0.93 at about 6000, 8000 and 11000 m behind the leading edge of the farm. In the following we shall see how close the different versions of the roughness change model can get to these figures

In roughness change models the wind farm is associated with a surface roughness as seen in Figure 5 and Figure 6 above.

In the roughness change models we associate the surfaces involved with surface roughness. Following the above figures, we assume two dimensional modelling, having to estimate roughness values for the water surfaces before and behind the wind farm and

for the wind farm itself. From standard formulations (Sempreviva et al., 1990) we take the basic water roughness as: z_{ow}= 0.0002 m.

The formula shown on Figure 5 expresses the wind farm equivalent surface roughness from the area averaged thrust coefficient, the hub-height and the background turbulence intensity. For the situations reflected in the figure above, we find the wind farm roughness to: z_{oWF} = 0.68 m.

The internal boundary layers in the roughness change model are assumed to grow as:

$$\frac{dh}{dx} = C\frac{u_*(h)}{U(h)},$$

where h is the height of the internal boundary layer growing from the roughness change point. u_* is the friction velocity and U is the mean speed. The surface friction within the new internal boundary layer is found by matching the up stream and the down stream wind speed at the height h. For the simplest case with two logarithmic profiles we find:

$$U_0(h_1) = \frac{u_{*0}}{\kappa}\ln(\frac{h_1}{z_{0w}}) = \frac{u_{*1}}{\kappa}\ln(\frac{h_1}{z_{0WF}}) = U_1(h_1),$$

where we have considered the growth of the internal boundary layer over the wind farm, when the up-stream over-water wind blows over the wind farm. It is seen that we can determine the down stream profile from the up-stream profile and the two roughness values.

The different roughness change models are characterized by different assumption about the profile formulation, the variation of u_* with height, different growth formulas for h and different estimates of the surface roughness. This does all sound quite arbitrary, but as we illustrate later the roughness changes models are actually quite robust. This is illustrated below using the simplest IBL modeling (based on surface layer and logarithmic profiles) for the wind behind the wind farm.

Using the notation from above, it is seen that the ratio between the wind speeds at hub height in front of the wind farm and behind it can be written for a given distance X.

$$\frac{U_2(h_{ub})}{U_0(h_{ub})} = \frac{\ln(\frac{h_1}{z_{0w}})}{\ln(\frac{h_1}{z_{0WF}})}\frac{\ln(\frac{h_2}{z_{0WF}})}{\ln(\frac{h_2}{z_{0w2}})}\frac{\ln(\frac{h_{ub}}{z_{0w2}})}{\ln(\frac{h_{ub}}{z_{0w}})}$$

Where we have basically used the matching of the two boundary layers twice rather than once, used before. The two heights, h1 and h2 refer to the two IBLs shown on Figure 5. The water roughness behind the wind farm can in general be different, as is indeed illustrated in the first part of this section 3.2. If the two water roughness values are just close, the last ratio in the equation is approximately one. The equation illustrates the robustness of the modeling, in that uncertainty on both the IBL heights and the roughness values tend to cancel.

Figure 8 shows the recovery of the wind behind the wind farm, according to the data above and from results from the basic surface layer model (SL) model with modified profiles and standard logarithmic wind profiles and with modified profiles, as described in (Sempreviva et al., 1990). We will not expect the model to provide useful results just

behind the wind farm (first data point), since the height of the new internal boundary layer developing behind the wind farm is much lower than the hub height. At the second point at 8 km, the IBL height, in the last IBL, is of the order of 450 m, and hence a roughness change model may work. At the last point at 11 km the roughness layer model should be best. The model is seen to shown somewhat faster return to upstream conditions than the data.

Figure 9 shows the behavior of the same SL model, where the roughness upstream roughness has been modified, following the WAsP methodology, where far upstream roughness values, here the wind farm roughness, converges exponentially towards a general background roughness, here the water roughness. Figure 10 illustrates that this approach indicates and even faster recovery of the wind behind the wind farm that the basic SL model. This is an expected result since the WAsP approach accelerates the return towards conditions over a free water surface by this exponential change of the wind farm roughness value.

In Figure 11, the roughness change model includes the behaviour of the internal boundary layers above the surface layer, with associated modifications of both the wind profiles and the turbulence level that is responsible for the growths of the IBLs. The effect of this modification is minor, and still the model predicts a faster recovery of the wind after the wind farm than does the data.

For this type of models it is important to characterize the turbulence that drives the growth of the IBLs involved in the model, since the turbulence structure of each IBL is different. It is normal to use the turbulence from the boundary layer with the strongest turbulence level as driver of the IBL growth In this case the strongest turbulence is associated with the largest roughness, that is the wind farm. However, after the wind farm this turbulence slowly decays leaving only the turbulence over the water surface to drive the continued growth of the IBL after the farm. In figure 11 this is modelled by having both IBLs grow with the wind farm turbulence until about 1 wind farm scale (5 km) downstream, where the final growth is taken over by the over-water –turbulence. This approach is seen to improve the prediction at the 11 km data point.

We therefore conclude a roughness change model may be modified to provide a reasonable match to the data, introducing a physically sensible modification. Additional work on the full data set will be performed to further evaluate this conclusion.

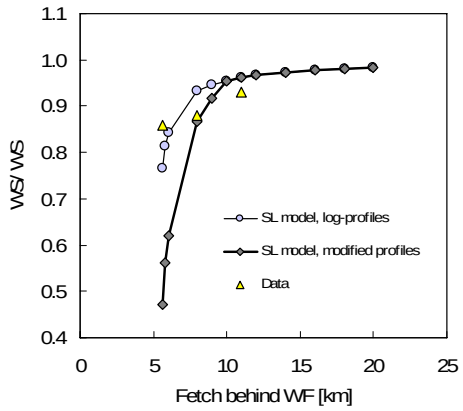

Figure 8 *SL roughness change model.*

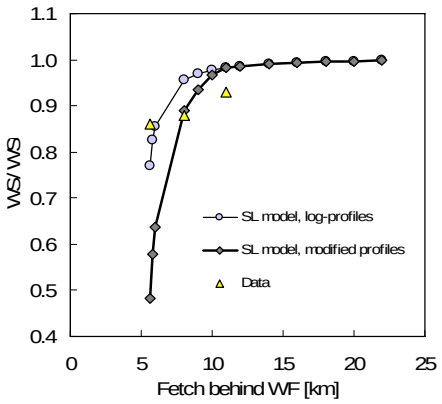

Figure 9 *SL roughness change model with WAsP roughness modification.*

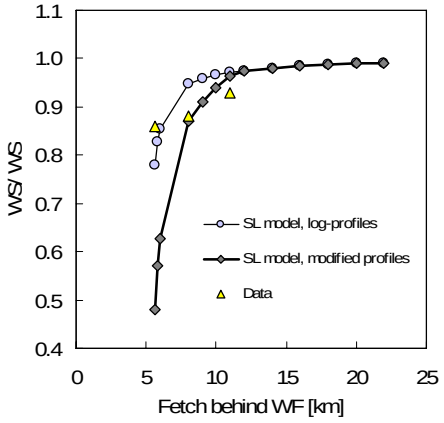

Figure 10 *Roughness change model including effect of boundary layer height.*

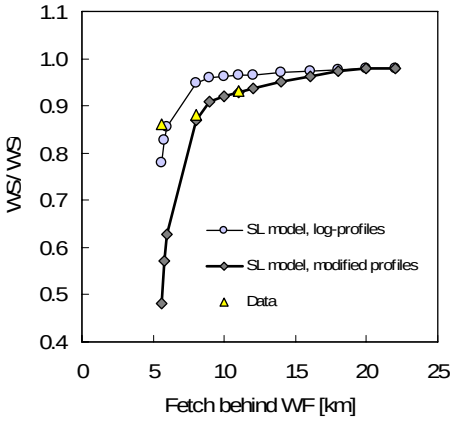

Figure 11 *Roughness change model with boundary layer heights and mixed.IBL growth.*

References

Gryning, S-E., Batchvarova. E., Brümmer, B., Jørgensen, H.E. and Larsen, S.E. , 2007: On the extension of the wind profile over homogeneous terrain byond the surface boundary layer. Boundary-Layer Meteorol. (article in press)

Sempreviva, A.M., Larsen, S.E., Mortensen, N.G. and Troen, I. (1990). Response of neutral boundary layers to changes of roughness. Boundary-Layer Meteorol., 50, 205--225.

3.3 Revised PARK model

The analytical model presented in Section 3.1 may only be implemented for wind farms with simple geometry. However, the model presented here is a generalized version of the analytical model.

The work has been directed to the development of a "Mosaic Tiles" model, where "Mosaic Tiles" refers to the pattern of more or less overlapping wakes at a certain down wind vertical plane in a wind farm wind. No linear approximations are applied in this model. The near-range wind flow around a turbine rotor is described be classical theory as depicted in Figure 12.

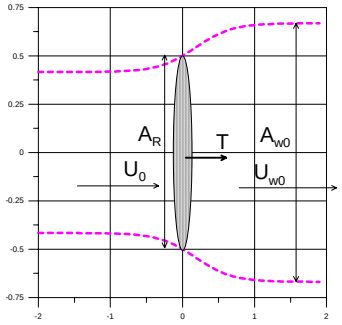

Figure 12. *Near range flow around the rotor.*

For each "Tile" (sub-area) in the "Mosaic", characterized as being covered by a single or a number of overlapping wakes originating from upwind turbines, the wind speed deficit is calculated from the balance equations for wind volume and momentum flow. The principle is illustrated in Figure 13 and Figure 14.

The individual turbine wakes are assumed to expand according to a power-law with an exponent 1/k between 1/3 and 1/2, but modified with abrupt expansions due to the local stream-line expansion around enshrouded turbines. This is described in the following equations for the wake diameter D_W in dependence if downwind distance x:

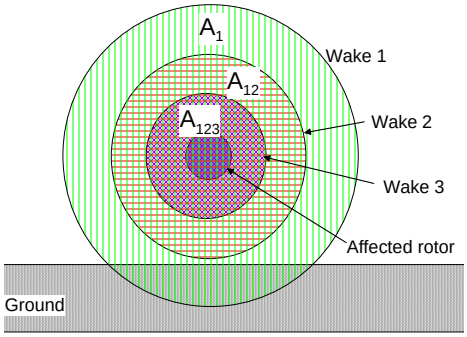

Figure 13 *Tiles in wake for straight row of wind turbines in line with wind direction.*

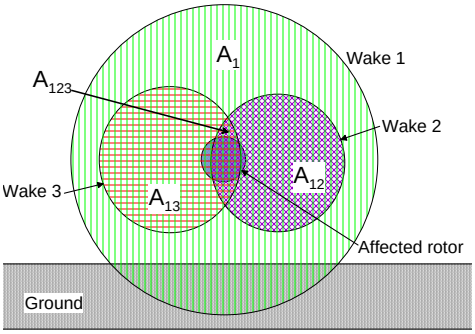

Figure 14 *Tiles for "arbitrary" wind farm geometry and wind direction.*

$$D_w(x) = D_R\left[\max\left(\beta^{k/2}, \alpha\frac{x}{D_R}\right)\right]^{1/k} \quad \Psi\ ,\ A_w(x_j, \Psi^{[j]}) - A_w(x_j, \Psi^{[j-1]}) = \Delta A_{T,j}$$

where β denotes the initial wake area relative to the rotor area and α is a dimensionless wake expansion parameter of the order of 1. Ψ is a parameter, which from an initial value of unity, steps up every time another downwind turbine "j" is passed, each step corresponding to the stream-line area-expansion $\Delta AT_{,}j$ around the downwind turbine.

The model parameters are to be determined by comparative predictions with data from Danish off-shore wind farms

The wake model with parameters 1/k = 1/3 and α=1.2 has been tested against data from the Horns Rev offshore Wind Farm in the North Sea West of Esbjerg, Figure 15.

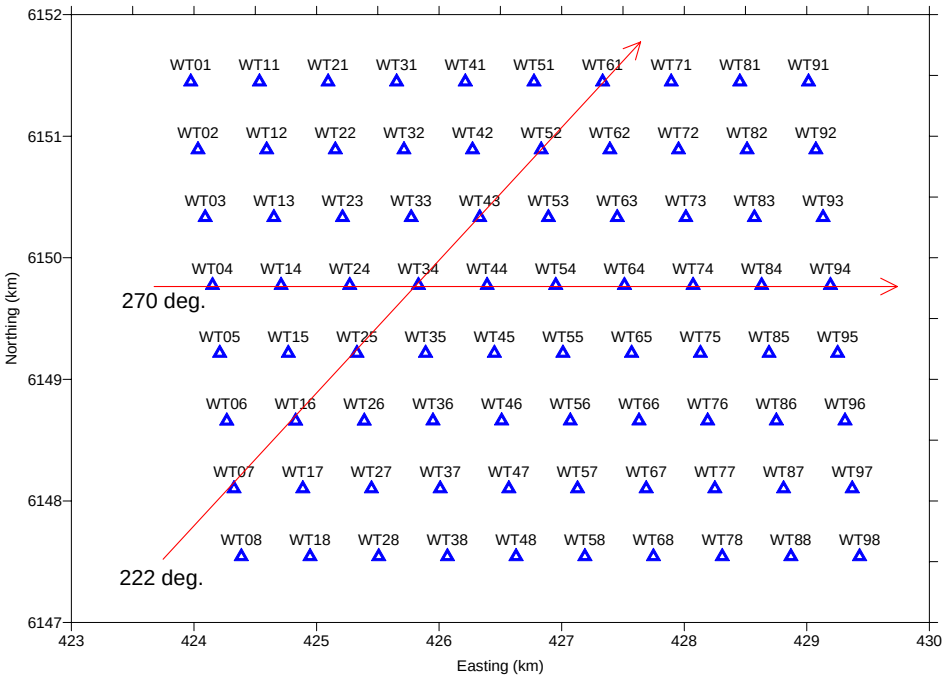

Figure 15. *Horns Rev Wind Farm Layout. 80 Vestas 2MW turbines. Rotor diameter: 80 m, Hub height: 70m. Spacing: about 7 rotor diameters.*

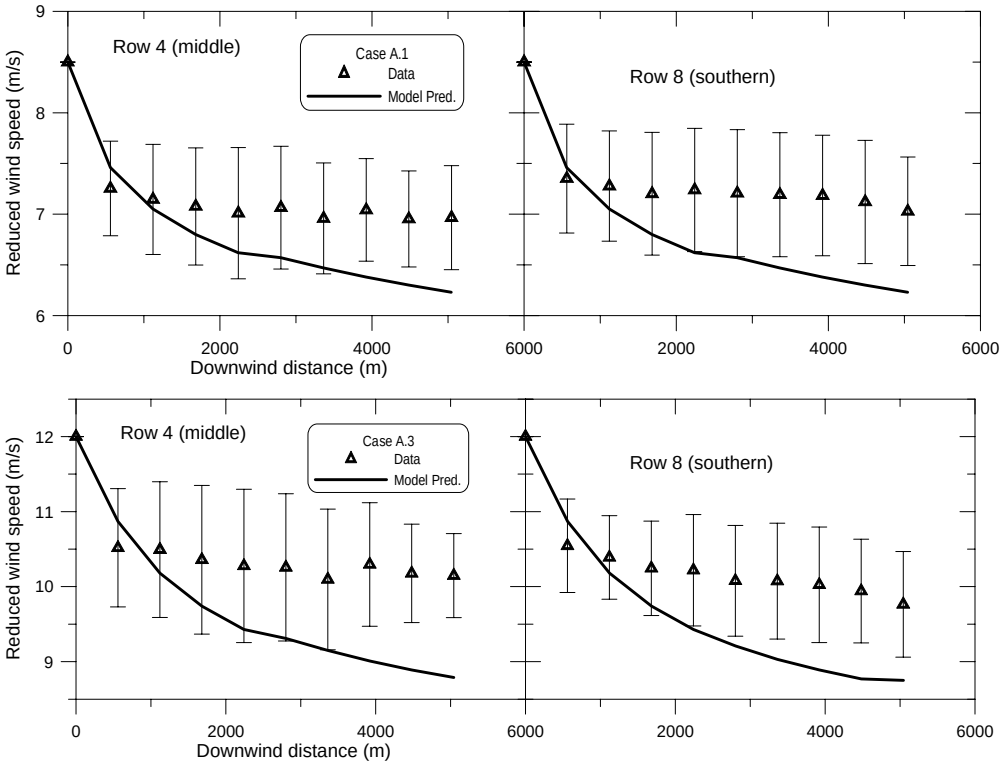

Figure 16. *Model predictions at wind direction 270° +/-3° compared to data. Free wind speed: 8.5 m/s +/- 0.5 m/s (top) and 12.0 m/s +/- 0.5 m/s (bottom).*

The wind directions along the main rows and the diagonal rows are indicated by arrows. Wind data with these directions were used when comparing to model results as shown in Figure 16 and Figure 17.

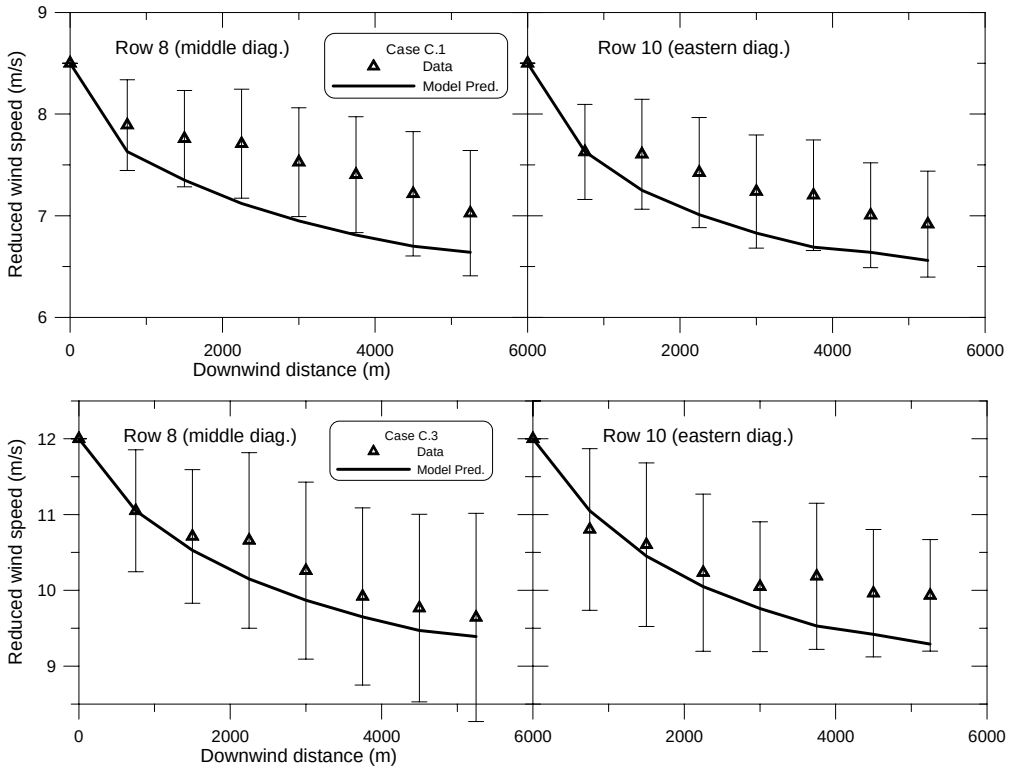

Figure 17. *Model predictions at wind direction 222° +/-3° compared to data. Free wind speed: 8.5 m/s +/- 0.5 m/s (top) and 12.0 m/s +/- 0.5 m/s (bottom).*

Clearly, whereas the present version of the mosaic-tile model is able to catch the level of the speed deficits correctly, it is not able to represent the experimental fact that – in the downwind direction - the wind speed drops markedly from the first to the second turbine but thereafter only drops insignificantly as you go further down wind the wind farm. Hence, the further development of the mosaic-tile wake model will be focused on adjustment of the model parameters (power-law exponent 1/k and the wake expansion coefficient α) based on comparisons with available data from Danish off-shore wind farms. This model adjustment will also allow for the parameters to not having fixed values but to depend on wind turbine operating characteristics (thrust and power) and on the wake overlapping.

3.4 Adopted Canopy model

In the following we have used the modelling concept introduce by Belcher et al 2003. The model concept is also very similar to that of Wasp and WaspEngineering. The models are all based on the linearization of the Navier-Stokes equations and only the perturbations of the flow (in this case the logarithmic profile) are modelled. In contrast to the roughness change models we have in this model introduced a volume drag force in both the x,y and z directions. The model is here only derived as 2D system but can easily be extended to 3D. Figure 18 illustrates the modelling domain where we have a background flow, which is logarithmic, over a small roughness, the wind farm which acts as drag force on the flow up till the height h with a characteristic drag length scale

L_c, and finally a domain where there is readjustment to the background flow. The closure to the turbulence modeling is illustrated in the figure. Here shown as a profile of the mixing length, which here is assumed to grow linearly with height, which again is in correspondence with the logarithmic background profile.

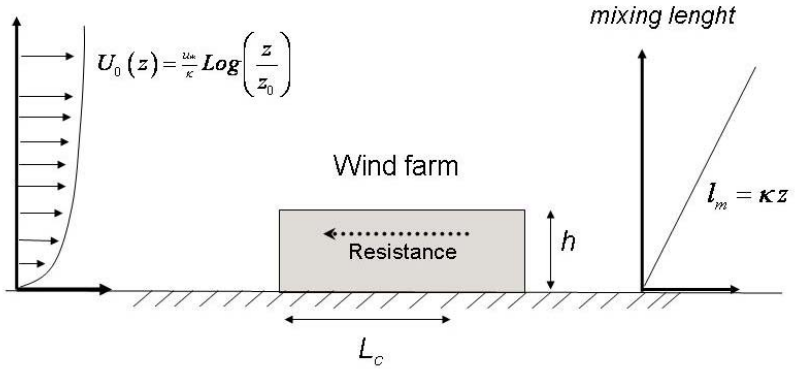

Figure 18 *Illustration of the model setup with a incoming windprofile and a wind farm which acts with a force on the incoming flow the height h is considerably higher than the roughness and therefore the modeling of the flow through the wind farm has to be established to predict how the flow behind the wind farm behaves.*

The model equations for the setup in **Error! Reference source not found.** then become:

$$U_j \frac{\partial U_i}{\partial x_j} + \frac{\partial P}{\partial x_i} = \frac{\partial \tau_{ij}}{\partial x_j} - f_i$$
$$\frac{\partial U_i}{\partial x_i} = 0 \qquad (1.1)$$

Here f_i is the drag force smoothed in time and space over the wind farm. U_i and P are the flow components also smoothed in time and space and τ_{ij} is the Reynolds stress tensor including the dispersive terms from the spatial smoothing.

The drag force F_i on a single object (i.e a wind turbine) can be modelled as:

$$F_i = \tfrac{1}{2} c_d A_t U_i |U| \qquad (1.2)$$

here c_d is the drag coefficient and A_f the area. We can now convert the force to a volume average over $h\ A_f$,and the volume force f_i then becomes:

$$\begin{aligned} f_i &= \tfrac{1}{2} c_d A_t U_i |U| / h A_f \\ &= U_i |U| / L_c \qquad (1.3) \\ L_c &= \frac{2h\ A_f}{c_d\ A_t} \end{aligned}$$

L_c is defined as the characteristic wind farm drag length scale of wind turbine park with the effective height h and the drag c_d corresponds to the thrust coefficient C_t. We can then express can L_c in terms of wind farm parameters as:

$$L_c = \frac{h\, s_r s_l\, 8}{\pi\, C_t} \qquad (1.4)$$

Here s_r and s_l are the distance between the columns and rows in the wind farm expressed in rotor diameters D.

We also need to model the shear stress tensor $\tau_{ij} = \langle u_i u_j \rangle$ which in terms of gradiants can be modelled as:

$$\tau_{ij} = l_m^{\,2} \sqrt{\left(\frac{\partial U_p}{\partial x_q} + \frac{\partial U_q}{\partial x_p} \right)} \frac{\partial U_p}{\partial x_q} \left(\frac{\partial U_i}{\partial x_j} + \frac{\partial U_j}{\partial x_i} \right) \qquad (1.5)$$

here the mixing length l_m is proportional to $l_m = \kappa z$ (please note that parts of the shear stress is absorbed in the divergence of the pressure, hence therefore not shown in (1.5)). Belcher et al. (2003) have assumed that the terms $\tau_{11} = \tau_{22} = \tau_{33} = 0$, but we have chosen to include all terms of (1.5). According to Belcher et al. (2003) the wind farm is considered as a weak forest and the mixing length approach with a linearly increase is appropriate.

The model equations (1.1) have been linearized and in following we have reduced the equations to 2D. Details of the linearization can be found WaspEngineering references. The equations are now reduced to:

$$\begin{aligned} U_0 \frac{\partial u}{\partial x} + w \frac{\partial U_0}{\partial z} + \frac{\partial p}{\partial x} &= \frac{\partial \tau}{\partial z} - f \\ U_0 \frac{\partial w}{\partial x} + \frac{\partial p}{\partial z} &= \frac{\partial \tau}{\partial x} \\ \frac{\partial w}{\partial z} + \frac{\partial u}{\partial x} &= 0 \end{aligned} \qquad (1.6)$$

By eliminating the pressure p and using the continuity equation (i.e. the last equation in (1.6)) we obtain the following equation for the perturbations w:

$$U_o \left(\frac{\partial^2 w}{\partial z^2} + \frac{\partial^2 w}{\partial x^2} \right) - \frac{\partial^2 U_0}{\partial z^2} w = -\frac{\partial^2 \tau}{\partial z^2} + \frac{\partial^2 \tau}{\partial x^2} + \frac{\partial f}{\partial z} \qquad (1.7)$$

This equation can now be Fourier transformed in x and we obtain the following:

$$U_o \left(\frac{\partial^2 \tilde{w}}{\partial z^2} + k^2 \tilde{w} \right) - \frac{\partial^2 U_0}{\partial z^2} \tilde{w} = -\frac{\partial^2 \tilde{\tau}}{\partial z^2} + k^2 \tilde{\tau} + \frac{\partial \tilde{f}}{\partial z} \qquad (1.8)$$

This equation is an ordinary differential equation which is solved numerical for each wave number k and the solution is transformed back into real space. Based on the continuity equation we can hereafter calculate the u perturbations and add them to the background flow which in this case is a logarithmic wind profile.

In the following we have calculated the effect of the Horns rev wind farm on the background flow. L_c has been estimated to approximately 15600 m but with comparisons between the measurements at Horns rev an appropriate value of 0.8 L_c has been chosen. The roughness outside the wind farm is set to z_o=0.0002 m and the background u_*= 0.33 m/s. The effective height is set to h = 100 m. The height of boundary layer is set to 500 m to limit the calculation domain. The solution is calculated for 64 different wave numbers. Here is should be stated that there is an analytic solution to the wavenumber k=0 which corresponds to the average wind profile for the whole of the domain. The resolution is chosen to 560 m

The results of the calculation are shown in Figure 19 and Figure 20. The first figure show the perturbations as function of height and downwind distance with respect to the logarithmic background profile. The wind farm is shown as the grey area around 16 km downwind from the start of the calculation and it here seen how the flow is blocked through the park and then accelerating to the background profile after the wind farm

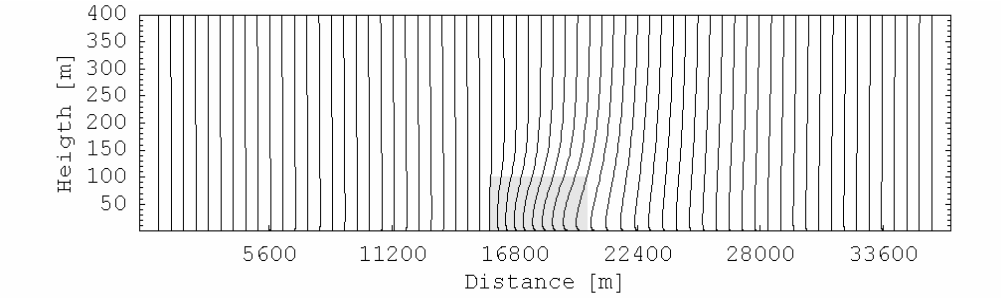

Figure 19 *The wind profile relative to background profile at different downwind distances. The gray area shows the location of the volume force which is distributed equal over this volume.*

In the last figure wind speed deficit at different heights are show normalized with the wind speed in front of the park. The solution is compared to the data from Horns rev and agrees very well. The solution has recirculating boundary conditions which also is seen in the solution.

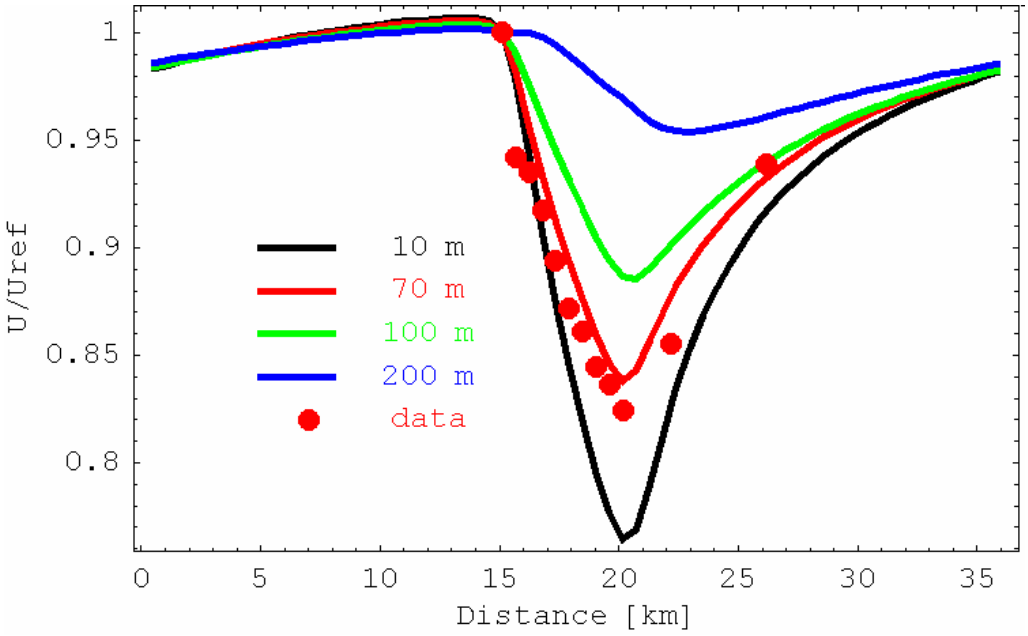

Figure 20. *Normalized wind speed through the wind farm and behind the wind farm compared to measurements at Horns rev.*

References

Belcher S.E., Jerram N., Hunt J.C.R (2003). Adjustment of a turbulent boundary layer to a canopy of roughness elements. JFM vol 488 pp 369-398.

3.5 MESO-SCALE model

In this section of work the mesoscale KAMM is used to model the flow at 50 m in the region around very large idealized offshore wind farms. The effect of the wind turbines on the flow is prescribed by a higher surface roughness than the surroundings. Different ways of distributing the same area of wind farm over a region are investigated; from using one large wind turbine group to using many smaller wind turbine groups. The results are presented by using mean wind speed maps of the wind farm region and transects of mean wind speed. The findings show the characteristics of the simulated wind reduction and recovery within and downwind of the wind turbine groups.

KAMM model. The Karlsruhe Atmospheric Mesoscale Model, known as KAMM, is a 3-dimensional, non-hydrostatic atmospheric mesoscale model (Adrian and Fiedler, 1991). It has it's origins in applications in regional flow and dispersion research.

The model can be used with its current set-up with a horizontal resolution down to about 2 km. The atmospheric flow is initialized using a forcing wind in geostrophic and hydrostatic balance. The forcing flow is prescribed by giving a vertical profile, using 4 different heights above sea level, of wind speed, direction and temperature. The forcing does not change in the horizontal direction.

Experimental configurations. For the mesoscale modelling a domain with a 2.5 km horizontal resolution is used. The domain size is 150 x 150 km in the horizontal and 5.5 km in the vertical. There are 25 model levels in the vertical and 61 x 61 cells in the horizontal directions. The entire domain has a surface elevation of 0 m; only surface roughness length, z_0, varies. The surface roughness length is set according to whether the

mesoscale model grid cell represents open water or open water and turbines. The surface roughness length for open water grid cells is 0.0002 m and for open water and turbines is 0.5 m.

Mesoscale model experiments using different configurations of wind farms grid cells and open water grid cells are performed. The different wind farm configurations represent the same total number of wind farm grid cells, and therefore the same sea area exploited for wind energy. The difference in the configurations is the grouping of the wind farm grid cells. The grouping ranges from having one big wind turbine group to having very many small wind turbine groups. The different wind farm configurations are shown in the below table.

Exp ID	Number of wind farms	Size of wind turbine group [km]	Distance between wind turbine groups[km]	Size of whole wind farm [km]	Total wind farm area [km^2]
1	1	30 x 30	-	30 x 30	900
2	4	15 x 15	15	45 x 45	900
3	9	10 x 10	10	50 x 50	900
4	16	7.5 x 7.5	7.5	52.5 x 52.5	900
5	36	5 x 5	5	55 x 55	900
6	144	2.5 x 2.5	2.5	57.5 x 57.5	900

Table giving details of the different wind farm configurations used in the mesoscale modelling. All the configurations have the same total area of wind farm, only the wind farms groupings differ.

The mesoscale model is forced by a climatological average profile defined by geostrophic wind speed, direction and potential temperature, calculated using the NCEP/NCAR reanalysis dataset over the period 1965 to 1998 for the location 11.25^{o}E 53.75 ^{o}N at the heights 0 m, 1500 m, 3000 m and 5500 m above sea level.

For each of the 6 wind farm configurations the forcing profile is used with 3 different wind directions, 260^{o}, 270 ^{o} and 280 ^{o}. The models is run for 6 hours of simulation time and then the model winds for model levels at 20.3 m and 58.7 m are interpolated to give the wind speed and direction at 50 m above sea level. The vector mean of the 50 m wind using the 3 direction simulations is calculated for each wind farm configuration.

Results. Figure 21 shows vector mean amplitudes and directions for the 6 wind farm configurations over the entire modelling domain. The wind direction is turned slightly anticlockwise relative to the forcing wind direction because of the surface friction acting on winds in the boundary layer producing the Ekman spiral. The effect of the higher roughness of the wind farm grid cells can be seen in the reduction in the wind speed downwind of the wind turbine groups. For the larger turbine groups, the reduction in the wind speed within the turbine group can also be seen. This effect gives a markedly lower wind speed for grid cells located along the downwind edge of the turbine group.

Figure 22 shows the mean wind speed for the 6 wind farm configurations along 61 transects of constant northing. Black and red lines show transects that do pass and transects that do not pass through the wind farm grid cells respectively.

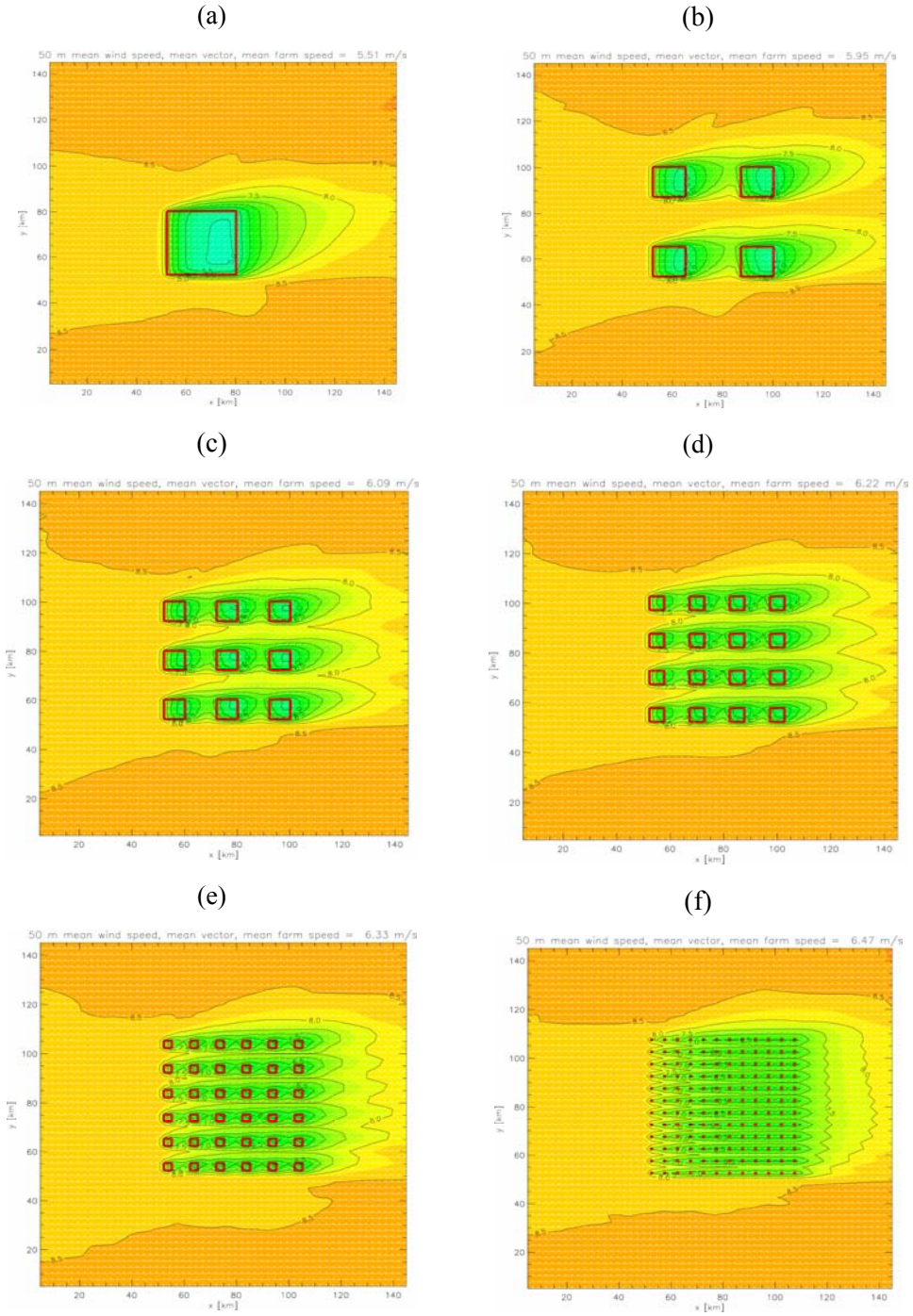

Figure 21. *Plots showing mean wind speed (colours) and vector wind (arrows) calculated for 3 simulations in the westerly sector, for each of the 6 wind farm configurations listed in the above table: Exp ID 1, (a), 2, (b), 3 (c), 4, (d), 5, (e), 6, (f). The red squares show the extent of the wind turbine groups in each configuration.*

For the transects that pass through the wind farm grid cells, a relatively abrupt reduction of the wind speed is seen as the flow enters the wind turbine group. The rate of reduction

decreases with distance into the turbine group. The wind speed inside the largest wind turbine group approaches an asymptote, at which point the wind farm grid cell roughness has lead to an nearly complete adjusted to steady wind profile.

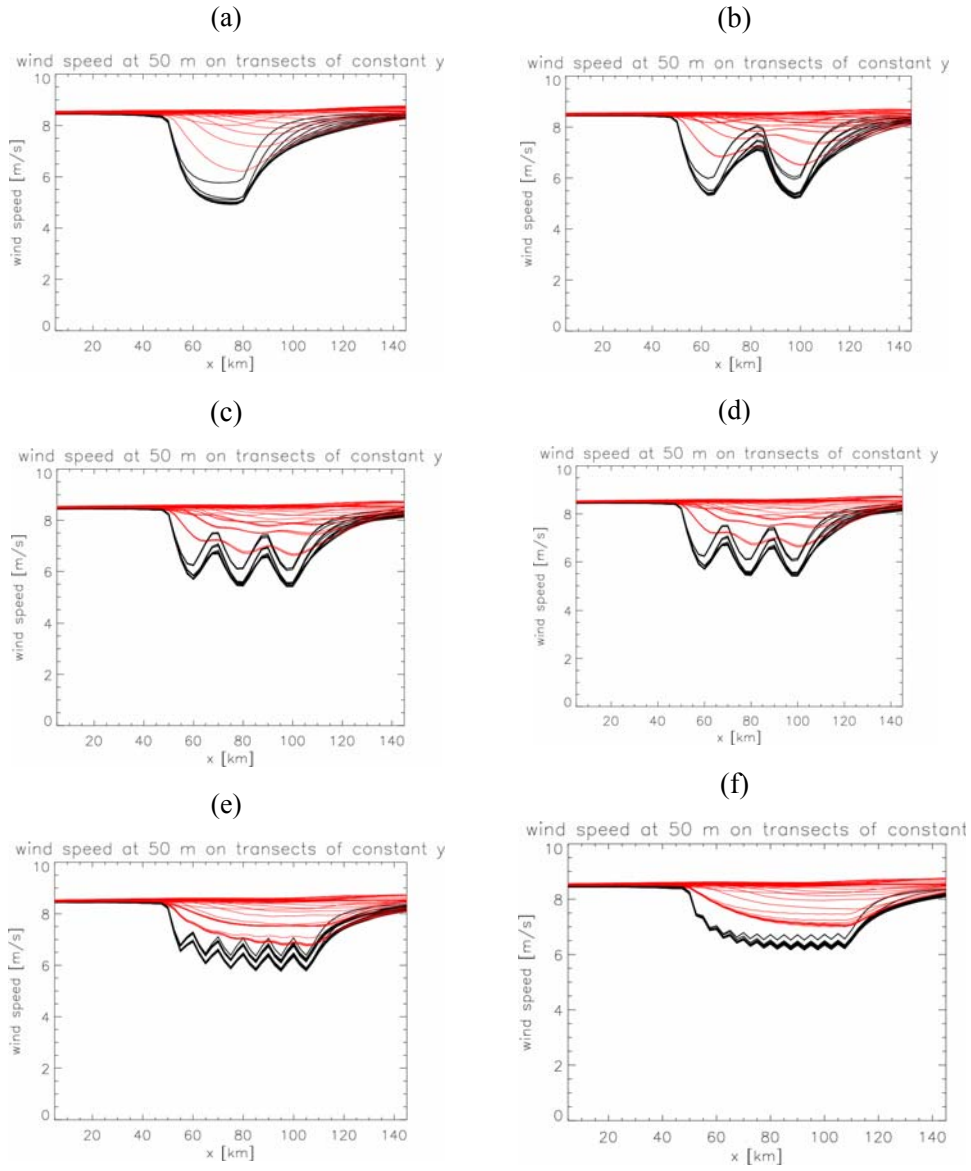

Figure 22. *Plots showing transects along constant northing of the mean wind speed calculated for 3 simulations in the westerly sector, for each of the 6 wind farm configurations listed in the table: Exp ID 1, (a), 2, (b), 3 (c), 4, (d), 5, (e), 6, (f). Black and red lines show transects that do pass and transects that do not pass through the wind farm grid cells respectively.*

Downwind of the wind farm cells the wind speeds increase steadily until the wind speeds observed upwind or far to the sides of the wind farm cells are approached. For the smaller wind turbine groups the recovery to the open water wind speeds is not reached, because the distance between turbine groups is too small. On the other hand the reduction of the wind speed is smaller for the smaller turbine groups.

Conclusions and discussion. This study has given mesoscale modelling results for a set of idealized wind farm configurations. The total wind farm area is fixed but the manner in which the wind turbines are grouped is varied.

The mean wind speed and mean vector wind is shown for 3 simulation for each wind farm configuration. The 3 simulation use different wind forcing directions (260^o, 270^o and 280^o) covering the westerly sector. The mean wind speed for wind farm grid cells is higher for smaller turbine groupings compared to larger turbine groupings. The approach to an asymptotic minimum wind speed within the largest turbine group takes approximately 20 km. The minimum wind speed within the turbine groups decreases in successive downstream turbine groups. For smaller turbine groups the successive downstream minimum wind speeds within the turbine groups also looks asymptotic. This suggests new effective roughness for clusters of small wind turbine groups.

The downstream wind speed recovery or wake decay looks similar in all configurations. Recovery to flow upwind of the turbine groups takes approximately 30 – 60 km. When the distance between turbine groups is small there is a reduced recovery. It is seen that the wake direction is similar to surface flow direction and this flow is turned slightly southerly, due to surface friction (Ekman spiral).

The mean wind speeds within the wind turbine groups give an indication of the production of the different farm configurations. Although the small groupings of turbines may give the best power production for a given number of turbines, the overall area used by the wind farm is larger. Therefore any further analysis to reach some kind of efficiency score of the different farm configurations needs a careful consideration of what quantity is to be maximized.

It would be of interest to investigate the assignment of different surface roughness to the wind farm grid cells, and to check the sensitivity of the results. Also of interest is to investigate if the decreased wind associated with the wind turbine groups is associated with a wind and wake turning. Investigation of alternative and improved ways to parameterize the effect of wind turbines on the flow will be required in order to apply more fully at higher resolution model results in this kind.

References

Adrian, G. and F. Fiedler, 1991: Simulation of unstationary wind and temperature fields over complex terrain and comparison with observations. Beitr. Phys. Atmosph. 64, 27-48.

Orlandski, I., 1976: A simple boundary condition for unbounded hyperbolic flows. J. Comp. Phys. 21, 251-269.

Klemp, J. B. and D. R. Durran, 1983: An upper boundary condition permitting internal gravity wave radiation in numerical models. Mon. Wea. Rev. 111, 430-444.

Blackadar, A. K., 1962: The vertical distribution of wind and turbulent exchange in a neutral atmosphere. J. Geophys. Res. 67, 3095-3102.

3.6 CFD modelling

Introduction. The method propose is an attempt to extend the data available from the offshore wind farm Horns Rev, using a Computational Fluid Dynamics (CFD) code. The outcome of this method is meant to give extra information to calibrate engineering models, which can then be used in a systematic way.

The basic idea of the method is to estimate the wind properties at the exit of a wind farm and to model the development of the wake downstream of the wind farm. The key element is how to specify the wind farm wake correctly at the computational inlet.

The data set available includes 3 meteorological masts surrounding the wind farm (one at a corner, and two aligned with a row of turbines, see Figure 1). The two aligned masts give an idea on how the wind is recovering from the influence of the wind farm, but with only two locations, no trends can be seen. The idea is to use these two met masts to "extrapolate" a trend of the wind speed recovery after the wind park.

A steady CFD code is used to model the wind exiting the wind farm. The domain modeled is beginning at the location of the first met mast downstream the park and is encompassing a large area downstream the wind farm, including the second met mast. The turbulence model used is the k-ε model, which implies that the inputs needed at the inlet are the mean wind speed U_{mean}, turbulent kinetic energy k, and dissipation distribution ε, the free stream friction velocity u_*, and the roughness coefficient of the sea z_0. All these parameters are estimated from the met masts measurements whenever it is possible, or, otherwise, derived from physical considerations.

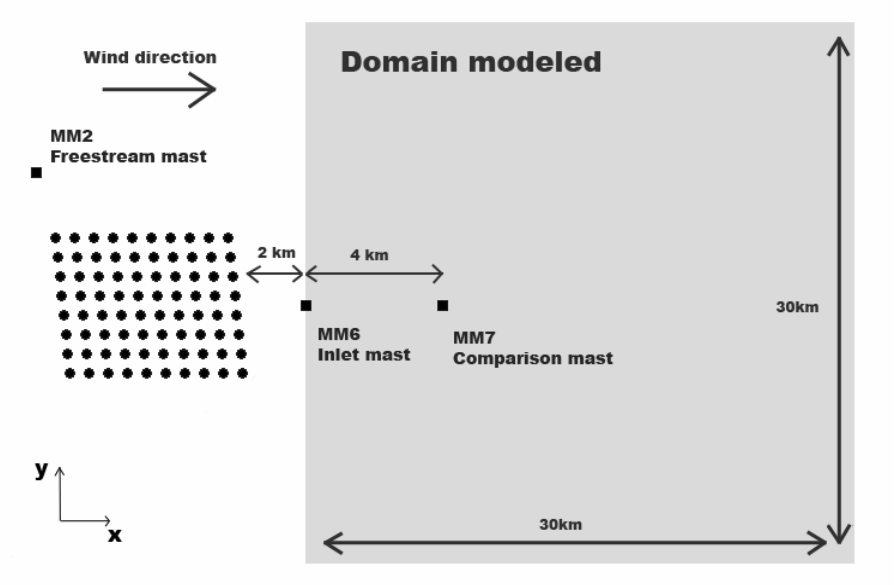

Figure 23. *Model Setup.*

The side boundary conditions are taken as symmetric, while the top boundary condition is taken as an inlet boundary, and the bottom as a wall boundary with a no-slip condition.

As previously mentioned, the inlet boundary is composed of two main regions, a free stream region, where the flow is assumed to be undisturbed by the wind farm, and a wake region, Figure 24.

The wake region is defined as a rectangle of 5km of width and 200m of height. In addition a linear transition region of 100m around the wake region is applied to smooth the resulting shear forces generating by the difference of wind speed from one region to another.

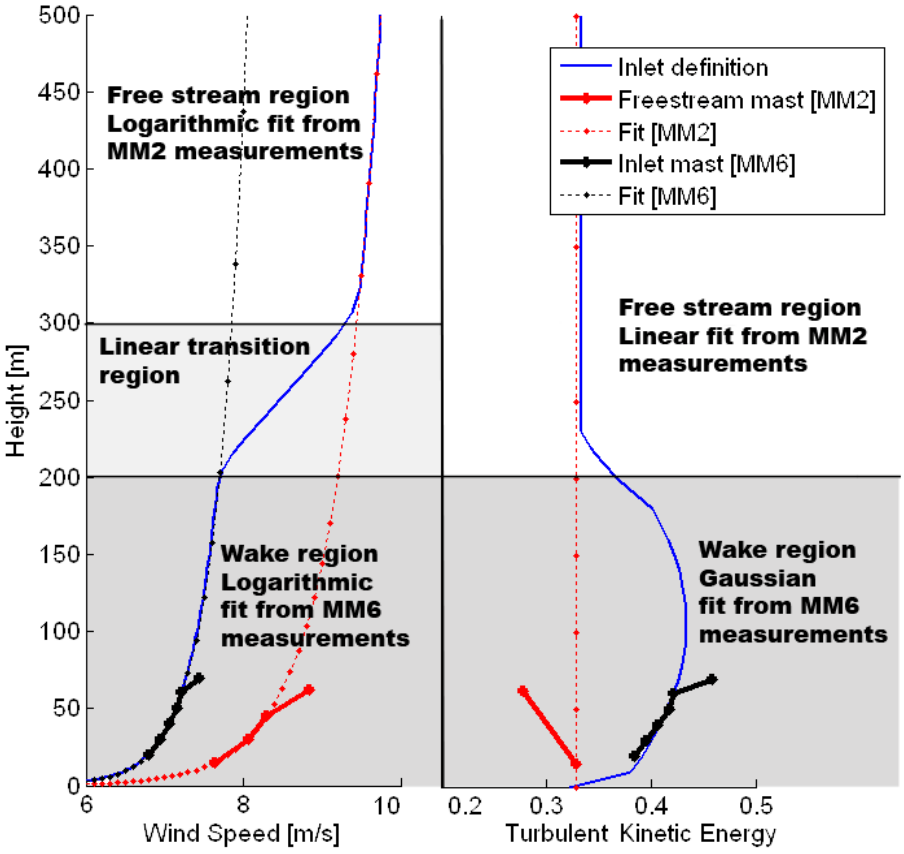

Figure 24. *Inlet specification*

Results. The vertical mean wind speed distribution 4km inside the domain seems in good agreement with measurements, Figure 25.

On the other hand the turbulence profile is largely different from the measurements, Figure 25. In addition the expected trend of the turbulence would be to decrease constantly instead of increasing as shown in Figure 26. This turbulence plot clearly shows the weakness of this model. As there is no physical model of the balance between mean wind speed profile and turbulence profile at the inlet, the arbitrary wind shear of the transition area yields a dramatic increase of the turbulent kinetic energy and dissipation until they reach a balance, and begin to decrease

Shortcomings and limitations of the method. The rate of the wake recovery is directly dependent on the prescribed turbulent kinetic energy and dissipation at the inlet. While the first one can be partly estimated from the available measurements, the second is totally unknown and requires a more detailed description.

Similarly, the transition area, defined as linear, is also unphysical. This high velocity gradient generates a high shear directly responsible for the unrealistic increase of turbulent kinetic. In order to avoid this jump, this transition area also necessitates a better specification of the turbulence profile.

For these reasons, without a proper physical wake definition of a wind farm, or more detailed information on the flow leaving a wind farm, the method still needs further investigation to obtain reliable results.

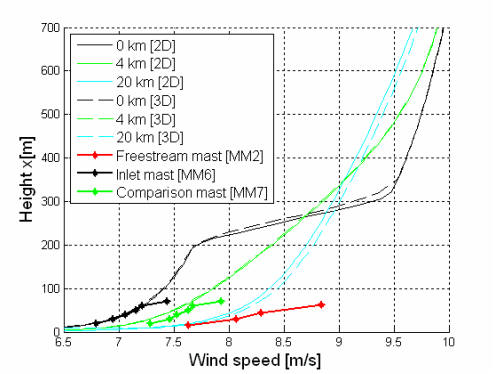

Figure 25. *Mean wind vertical profile in the center plane of the domain*

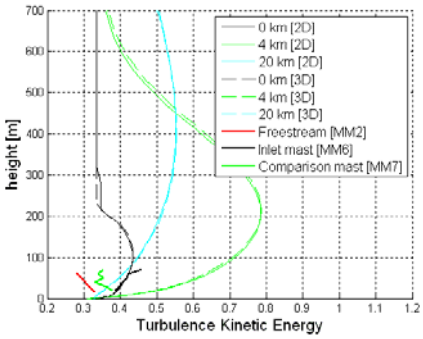

Figure 26. *Turbulent kinetic energy vertical profile in the center plane of the domain*

4 Project-generated publications

Barthelmie, R.J., Frandsen, S., Pryor, S. and Landberg, L. 2005: Wakes within and downwind of large offshore wind farms. *American Wind Energy Conference,* Denver, May 2005.

Barthelmie, R.J., Giebel, G., Jorgensen, B.H and Badger, J. 2005: Short-term forecasting of wind speeds in the offshore environment. *'Copenhagen Offshore Wind 2005',* Copenhagen, October 2005.

Barthelmie, R., Frandsen, S., Jensen, L, Mecali, M. and Rethore, P. 2005: Verification of efficiency model for very large wind turbine clusters, *'Copenhagen Offshore Wind 2005',* Copenhagen, October 2005.

Barthelmie, R., and Giebel, G. 2006: Prediction of wind speed profiles for short-term forecasting in the offshore environment. *European Wind Energy Association Conference*, Athens, Greece, February 2006.

Barthelmie, R.J., Frandsen, S.T., Nielsen, N.M., Pryor, S.C., Rethore, P.E. and H.E. Jørgensen, 2006: Modelling and measurements of power losses and turbulence intensity in wind turbine wakes at Middelgrunden offshore wind farm, *Wind Energy*.

Barthelmie, R.J., Pryor, S.C. and Frandsen, S.T. 2006: Climatological and meteorological aspects of predicting offshore wind Energy*, Offshore Wind Book,* eds: G. Gaudiosi and J. Twidell).

Barthelmie, R.J., Frandsen, S.T., Rethore, P.E., Mechali, M., Jensen, L. and Sørensen, P., 2006: Power losses from wakes: issues in modelling and measurements. *British Wind Energy Association Conference*, Glasgow, Scotland, October 2006.

Frandsen, S, R. Barthelmie and O. Rathmann, 2007: Wake Modelling for intermediate and large wind farms, EWEC 2007

Barthelmie, R., Folkerts, L., Larsen, G., Pryor, S.C., Frandsen, S.T. and Schepers, G. 2006: Comparison of wake model simulations with offshore wind turbine wake profiles measured by sodar, *Journal of Atmospheric and Oceanic Technology***, 23(7),** 888-901.

Frandsen, S.T., Barthelmie, R.J., Pryor, S.C., Rathmann, O., Larsen, S. Højstrup, J. and Thøgersen, M. 2006: Analytical modelling of wind speed deficit in large offshore wind farms. *Wind Energy ,* **9**, 39-53.

Barthelmie, R.J., Frandsen, S.T., Mechali, M., Jensen, L., Sørensen, P., Rethore, P.E. and Mann, J. 2006: Wakes in large wind farms, *European Geophysical Society Annual Conference*, Vienna, April 2006. EGU06-A-01401 (poster). *Geophys. Res. Abstr. (CD-ROM)* (2006) **8** (no.Abstr. EGU06-A-01401).

Barthelmie, R.J., Frandsen, S.T., Rethore, P.E., Pryor, S.C., Mechali, M., Jensen, L. and Sørensen, P. 2006: Modelling and measurements of offshore wakes. *Offshore Wind Energy in Mediterranean and Other European Seas, Rome, April 2006.* 31-43.

Barthelmie, R.J., Frandsen, S.T. and Nielsen, M. 2006: Modelling and measurement of wake generated turbulence at Middelgrunden. *Offshore Wind Energy in Mediterranean and Other European Seas, Rome, April 2006.* 45-53.

Badger, J., Barthelmie, R., Frandsen, S. and Jørgensen, B.H. 2006: Mesoscale modelling for an offshore wind farm, *European Wind Energy Association Conference*, Athens, Greece, February 2006.

Rathmann, O., Frandsen, S. and Barthelmie, R.: Wake Modelling for intermediate and large wind farms, *European Wind Energy Association Conference*, Milan, Italy, May 2007.

Mechali, M., Barthelmie, R., Perstrup, C., Frandsen, S., Jensen, L., Mørch, C. and Rethore, P.E. 2006: Wake effects at Horns Rev and Nysted and their influence on energy production. *European Wind Energy Association Conference*, Athens, Greece, February 2006.

Jensen L. E., L. E., C. Mørch, P. B. Sørensen, K. H. Svendsen 2004: Wake measurements from the Horns Rev wind farm, EWEC2004, London.

Larsen, S.E., 2007, Offshore Meteorology. Symposium: Decentralised energy systems-Integrated renewable energy technologies in tomorrow's energy supply, Oldenburg (DE), 15-16 Feb 2007.

Rathmann, O., Barthelmie, R. and Frandsen, S. 2006: Wake model for wind farm power production. *European Wind Energy Association Conference*, Athens, Greece, February 2006.

Réthoré, P.-E., Bechmann, A., Sørensen, N.N., Frandsen, S.T., Mann, J., Jørgensen, H.E., Rathmann, O. and Larsen S.E. 2007: A CFD model of the wake of an offshore wind farm: using a prescribed wake inflow. *The Science of making Torque from Wind, Second Conference*, Technical University of Denmark, Lyngby, Denmark, August 2007.

Risø's research is aimed at solving concrete problems in the society.

Research targets are set through continuous dialogue with business, the political system and researchers.

The effects of our research are sustainable energy supply and new technology for the health sector.